



# Development of an UV rolling system for fabrication of micro/nano structure on polymeric films using a gas-roller-sustained seamless PDMS mold

Yun-Heng Lee<sup>1</sup> · Kun-Cheng Ke<sup>1</sup> · Nai-Wen Chang<sup>1</sup> · Sen-Yue Yang<sup>1</sup> 

Received: 23 October 2017 / Accepted: 18 December 2017 / Published online: 2 January 2018  
© Springer-Verlag GmbH Germany, part of Springer Nature 2018

## Abstract

Roller imprinting is one of the most effective methods to fabricate polymeric plate components with nanostructures on the surface. In this study, a gas-bag roller is employed to increase the contact area and ensure conformity of contact between the roller mold and the substrate. The gas-bag roller has a seamless polydimethylsiloxane (PDMS) roller mold with a nanopillar array. Most of the replicated patterns are not continuous because of roller mold with seams, therefore, the seamless roller mold was produced by PDMS and used to imprint the patterns in this research. Micro/nano-structures were fabricated by casting into the micro/nano-pores of the anodic aluminum oxide (AAO) roller. The micro/nano-pores in the AAO roller are made by a two-step anodization process from a circular aluminum tube of 99.9% purity. An UV-based imprinting facility integrating a gas-bag roller and PDMS roller mold were designed and implemented to replicate nanostructures on the surface of the polycarbonate (PC) continuously. The antireflection and the hydrophobic effects of the fabricated PC film were verified. The reflection drops from 14.7% in the bare PC film to 2% in the PC film, and the contact angle increases from 77.5° in the bare PC film to 124.1° in the PC film with nanostructures.

## 1 Introduction

Nanostructured thin films have been widely used in applications such as bio-sensing (Bantz et al. 2011), self-cleaning (Chuang et al. 2013) and anti-reflective components (Päivänranta et al. 2008). Most commercial nanostructures have been fabricated on the surface of polymeric films or plates by injection molding (Matschuk and Larsen 2013) or hot embossing (Wen et al. 2011) from an electroplated mold. Injection molding has difficulty manufacturing surface-structured large thin plates, due to the large flow resistance and induced residual stress. On the other hand, hot embossing replication has problems such as non-uniform pressure, long heating and cooling cycle times. To reduce the embossing pressure and heating/cooling time, UV resin imprinting technology was developed (Park et al. 2009; Ahn et al. 2006, 2007; Lee et al. 2006; Ahn and Guo 2009; Wu and Yang 2010). For fabricating nanostructures

on polymeric substrates (plates or films), the nano-imprinting process has drawn great attention (Tan et al. 1998; Mäkelä 2008).

In recent years, there has been an increasing interest in the study of superhydrophobic surfaces, due to their potential applications in, for example, self-cleaning, nanofluidics, and electrowetting (Fei et al. 2008; Guldin et al. 2013; Nanayakkara et al. 2010). The possibility of making high-contact-angle, rough surfaces from low-contact-angle materials has recently been suggested and demonstrated. How to fabricate a high-contact-angle structure with an efficiency method become a trend and challenge. Generally, The Gibbs energy of a drop on a rough surface depends on two independent variables: the extent of penetration into the roughness valleys and the geometric apparent contact angle of the drop. These two variables must be considered simultaneously when determining the minimum in the Gibbs energy, that is, the equilibrium state (Marmur 2008). Therefore, the geometry and roughness of the surface could change the hydrophobicity critically.

Continuous roller imprinting is developed especially for mass production for replicating surface micro/nano structures at rapid speed and low-cost. There are two aspects of

✉ Sen-Yue Yang  
syyang@ntu.edu.tw

<sup>1</sup> Department of Mechanical Engineering, National Taiwan University, Taipei 106, Taiwan

challenges: the roller mold and the contact between the roller mold and substrate. Roll to roll imprinting is mostly used for the surface patterning of large, thin sheets, i.e. ceaseless products, which are often also produced by continuous processes such as extrusion and drawing, e.g. of foils and fibers. The roller mold is usually prepared by wrapping the electroplated nickel sheet on the roller (Gale 1997). However, there's a disadvantage of the roll to roll imprinting process, which is the mold wrapped on the roller may have seams. The stability of the mold and the existence of the seam are of constant concern. Most roller molds may have this problem due to the process of making the master mold occurs by plate to plate imprinting first, then wrapping it on the roller. This process will make seams which allow some pattern imprinting failure during the roll to roll imprinting (Unno and Taniguchi 2011; Dumond et al. 2012). Further, the contact between the roller and the substrate is nearly a line, with only a little contact area and brief time for replication and UV exposure; this prevents increasing the speed of imprinting (Park et al. 2009). A belt type mold was proposed to increase the contact area which can effectively enhance the speed of the roller, but the imprinting pressure is not uniform because the contact relies only on the belt tension between two rollers and the normal stress under two rollers (Ahn and Guo 2009). The PDMS belt mold with micro dots was wrapped into a gas-bag roller in UV imprinting (Wu and Yang 2010) to improve the contact and enhance the imprinting pressure uniformity. However, the stability and the endurance of the belt PDMS mold are suspected.

Anodic aluminum oxide (AAO) is used to cast a PDMS soft mold. AAO is a low cost mold, which is easy to produce. It is produced by the anodization of aluminum, which is an electro-chemical process that changes the surface chemistry of the metal, via oxidation, to produce an anodic oxide layer. During this process a self-organized, highly ordered array of cylindrical shaped pores can be produced with controllable pore diameters, periodicity and density distribution (Poinern et al. 2011). When high purity aluminum is anodized in an acidic electrolyte, a porous alumina membrane with uniformly parallel pores and straight walls is formed (Hwang et al. 2002). This enables the AAO membranes to be used as templates in various nanotechnology applications without the need for expensive lithographical techniques.

In this study, an effective, fast, and low-cost method to fabricate a seamless circular PDMS mold with nanostructures is proposed and developed. The PDMS soft mold is cast from the AAO roller template. In addition, a gas-bag roller-assisted UV imprinting facility is designed and implemented, to facilitate the circular seamless PDMS mold for replicating nanostructures continuously without defects on the surface of the PC film. The gas-bag roller

can increase the contact area and ensure the conformity of contact between the mold and the substrate. Nanostructures are successfully fabricated on PC film, which shows anti-reflection and hydrophobic effects.

## 2 Experiment setup

### 2.1 Fabrication of circular AAO master mold

An aluminum pipe with purity of 99.9% (Ultimate Materials Technology Co., Ping Tung, Taiwan) is used as the substrate for anodization. The outer and inner diameters are 66 mm and 60 mm respectively, and the length is 50 mm. To ensure only the inner wall of the pipe is immersed in the electrolyte, the outer surface of the pipe was isolated with the water-proof tape. The aluminum pipe is used as the anode, while a carbon tube is used as the cathode. The electrolyte is 0.1 M phosphoric acid solution in the first anodization. The anodization voltage is 180 V and the process time is 5 h. Following the first anodization, the anodic alumina layer on the substrate is removed using 1.22 M phosphoric acid at 32 °C. The second anodization is then carried out with the same parameters as in the first anodization. The process time is 3 h. Finally, the aluminum pipe is placed in 1.22 M phosphoric acid to widen the pores for 15 min. The SEM micro-photos at four different locations, as shown in Fig. 1, demonstrate their angle independency.

The pore formation, interaction between Al film and electrolyte result in the development of penetration paths from the external Al film surface. Since mobile  $\text{Al}^{3+}$  ions are lost to the electrolyte without forming solid metal, and there are no mechanisms to compensate for the internal penetration path, the porous anodic film is formed.

According to some previous papers (Poinern et al. 2011; Thompson 1997), various purities cause different uniformity of pores. The use of high purity Al foil allows the formation of periodical pores at a large-scale. In this work, the Al tube with a purity of 99.9% is employed, which can create structure on its surface. The purity of Al material is 99.9% with other elements, such as Si, Cu, Mg and Zn elements. These elements will self-organize micro/nano patterns and structure on the Al's surface during the process of making AAO.

### 2.2 Fabrication of seamless PDMS circular mold with micro/nano-structures

PDMS (Sylgare 184, Dow Corning, Midland, MI, USA) casting is employed to fabricate the micro/nano structures directly from the circular AAO master mold. There are two steps in this process, as shown in Fig. 2.

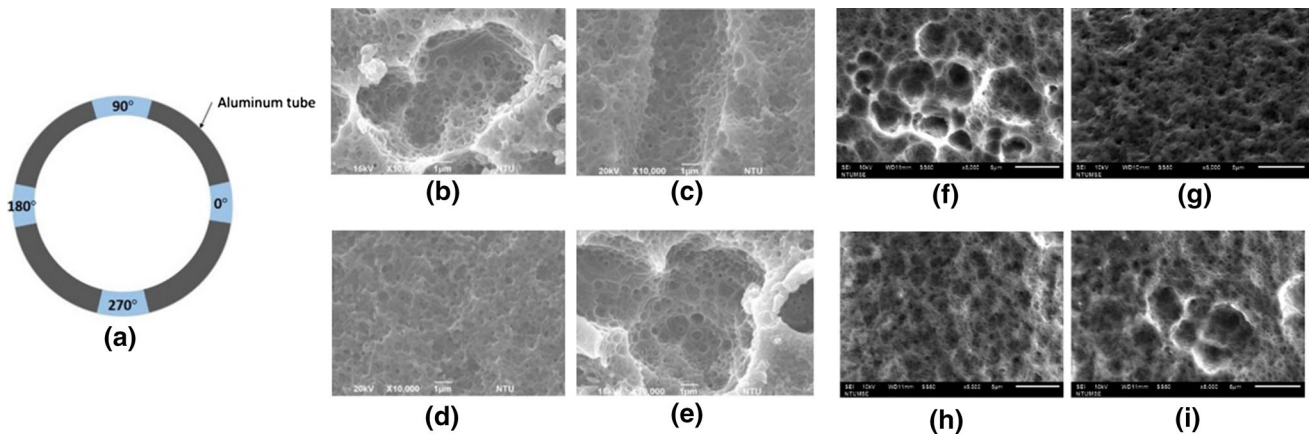


**Fig. 1** **a** Four locations on aluminum tube and SEM images of the micro/nano-pores circular AAO mold in four consecutive locations 90° apart. **b** 0°, **c** 90°, **d** 180°, **e** 270°; SEM images of the micro/nano-

pores circular PDMS mold in four consecutive locations 90° apart. **f** 0°, **g** 90°, **h** 180°, **i** 270°

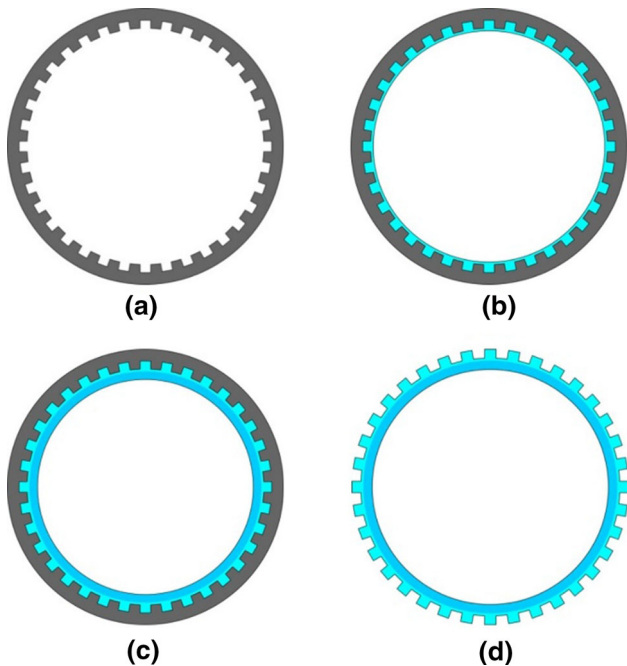


**Fig. 2** Schematic drawings showing the steps of casting the manufacturing of the seamless nano-structured circular PDMS mold from the inner wall of an AAO tube. **a** AAO master mold. **b** The first step of casting (using less-viscous PDMS). **c** The second step of casting. **d** Circular PDMS mold

The first step is to fabricate the AAO micro/nano-structures by filling the nano-poles with a less-viscous PDMS solution, which is prepared by mixing the 5.4 M toluene into the PDMS solution (weight ratio of the base agent and the curing agent 10:1). Heating is then applied to evaporate the toluene and cure the PDMS. This process is repeated until the inner surface of the aluminum pipe is covered with PDMS. The next step is the casting of a normal PDMS solution until a final thickness of 3 mm is reached. The circular PDMS ring is cured at room

temperature for 24 h. A circular PDMS ring (60 mm OD and 54 mm ID) with nano-pillar arrays can be obtained. It will be supported by a gas-bag roller, as explained in the following section.

### 2.3 Gas-bag roller-assisted UV imprinting facility

A gas-bag roller-assisted UV imprinting facility is designed and constructed for the experiments involving fabrication nanostructures onto polymeric substrates. As shown in Fig. 3, the facility consists of a gas-bag roller, two pneumatic cylinders, a moving platform and a UV lamp. The gas-bag roller is prepared by wrapping and sealing a silicon tube around an aluminum dumbbell-shaped roller, as shown in Fig. 4. The gas-roller is inflated to a specific gas

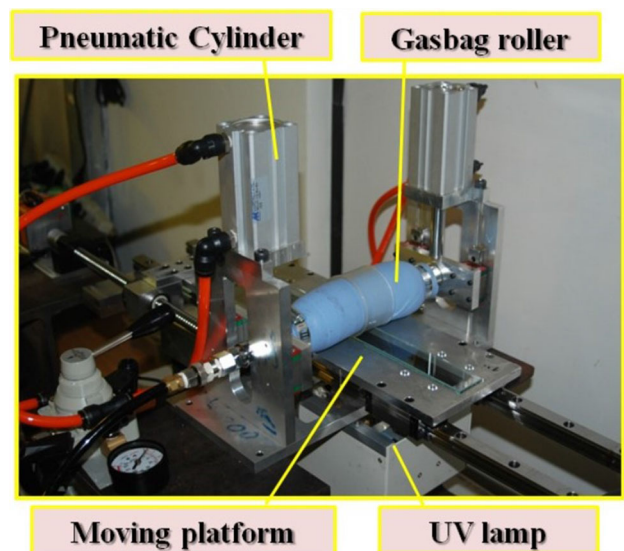
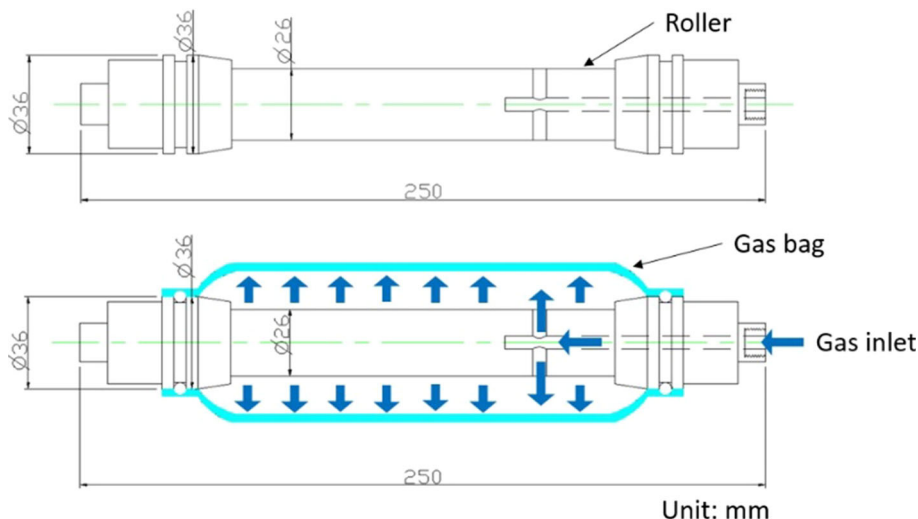


**Fig. 3** Photograph showing the gas-bag roller-assisted UV-based imprinting facility

**Fig. 4** Engineering drawing showing the components of the gas-bag roller



pressure, which is supplied by an air compressor and regulated by a pressure valve. The gas-bag roller expands and sustains the circular PDMS mold with the AAO nanostructures. The gas-bag roller can exert pressure over a certain contact area, not a line. The two pneumatic cylinders apply external pressure on the shaft of the gas-bag roller. The moving platform is driven by a lead screw and a motor. The operating procedure is shown in Fig. 5. The power of the UV lamp (UV-A365, Philips, Amsterdam, The Netherlands) is 400 W/cm<sup>2</sup>. The wavelength range of the UV light is 365–410 nm. The experimental process is shown in Fig. 6.

### 3 Results and discussion

#### 3.1 Comparison of the contact area and pressure uniformity using the gas-bag roller and rigid roller

Pressure sensitive films (PSF, 4LW, Fuji, Japan) are employed to measure the contact lengths in systems using the gas-bag roller and rigid roller. At a static condition, under specific pressure applied on the two ends of the roller shaft, as shown in Fig. 5, the red spots on the imprinted PSFs show the contact lengths with the gas-bag roller and rigid roller. Under the same outer gas pressure (0.5 kgf/

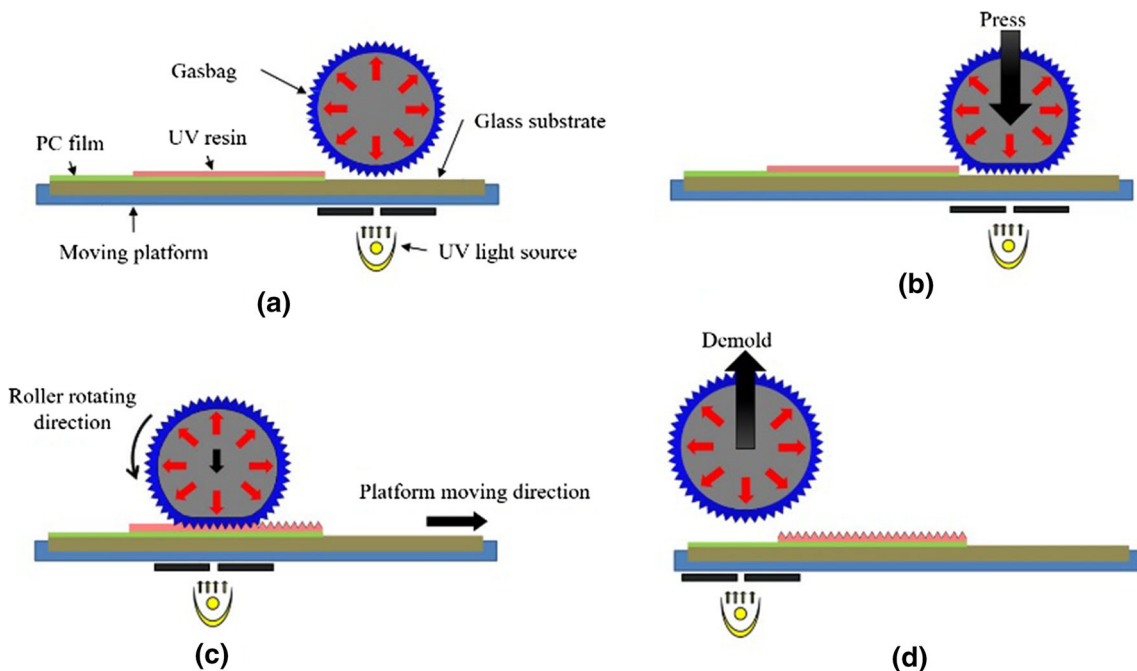


**Fig. 5** Schematic showing the gas-bag UV curing process **a** preparation, **b** pressing, **c** platform moving, **d** demolding



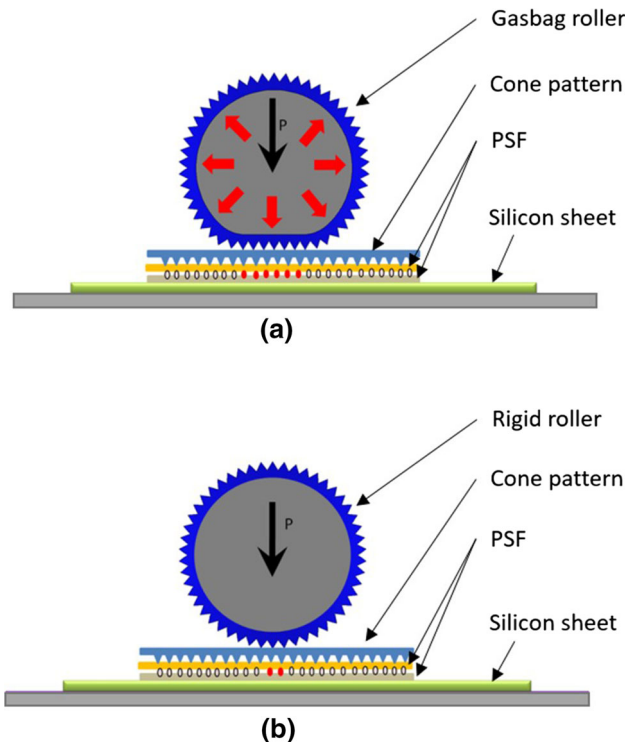


**Fig. 6** Measurement of the static contact area with the aid of pressure sensitive film using **a** gas-bag roller and **b** rigid roller

cm<sup>2</sup>), the contact length is 15 mm with the gas-bag roller, as shown in Fig. 7. With the gas-bag roller, the contact length increases with the outer pressure; the contact length

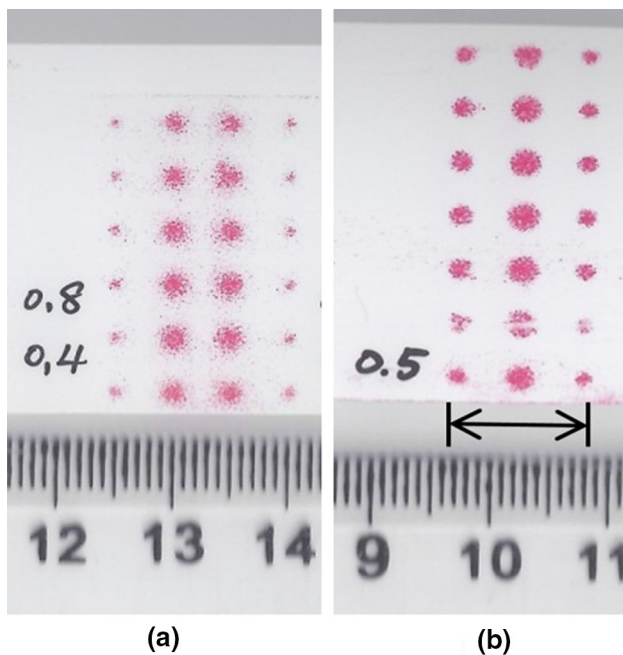


**Fig. 7** The measured static contact areas in systems using **a** gas-bag roller and **b** rigid roller

is not affected by the applied pressure with the rigid roller. A longer contact length implies more time for the UV resin (UV3215-B, Chem-Mat Technologies Co., CA, USA) to fill the cavities.

The pressure uniformity in systems using the two different rollers is compared as well. Under the same outer gas pressure (0.5 kgf/cm<sup>2</sup>), with the platform moving at the same speed, as shown in Fig. 8, the red spots are more uniform with the gas-bag roller than with rigid roller. This proves the gas-bag roller provides stable and uniform imprinting pressure.

### 3.2 Effect of imprinting conditions on the fabrication of micro/nanostructures using gas-bag rollers

The two main parameters in gas-bag rolling imprinting are the inner gas pressure and outer gas pressure. The inner gas pressure determines the elasticity of the roller, while the outer gas pressure determines the applied force on the two ends of the roller shaft. The proper range for the inner gas pressure is found to be 0.7–1.1 kgf/cm<sup>2</sup> and the outer gas pressure is 0.3–0.6 kgf/cm<sup>2</sup>. The operational window for fabrication of the nanostructure is shown in Fig. 9. If the inner gas pressure is too small, the gas-bag roller will not be able to sustain the PDMS mold, resulting in sliding between the mold and the gas-bag roller. If the inner gas pressure is too high, not only the roller becomes rigid, but also the circular PDMS mold will be distorted, and even broken. When the outer gas pressure is lower than 0.3 kgf/cm<sup>2</sup>, only the microstructures, but not the nano-pores, are replicated. Since the pressure is too low to force the filling of the nano-sized cavity, when the outer pressure is higher than 0.6 kgf/cm<sup>2</sup>, the friction prevents the platform from moving smoothly. Besides, a high pressure may deform or even distort the PDMS mold.

With the inner gas pressure of 0.8 kgf/cm<sup>2</sup>, outer gas pressure of 0.5 kgf/cm<sup>2</sup>, and platform moving speed of 0.145 mm/s, micro/nano structures are fabricated on the PC film (Lexan8010, GE, CT, USA) with a thickness of 178 μm and dimensions of 35 mm width and 230 mm length. Figure 10 shows the nano-structure can be completely fabricated on the PC film. This proves using seamless PDMS mold sustained with the gas-bag roller, AAO nanostructures can be fabricated on polymeric films.

### 3.3 The anti-reflective and hydrophobic properties of the fabricated PC film with micro/nano structures

The reflectance of a PC film coated with UV resin and a PC film with micro/nano-structures are measured at a wavelength between 300–800 nm. As shown in Fig. 11, the

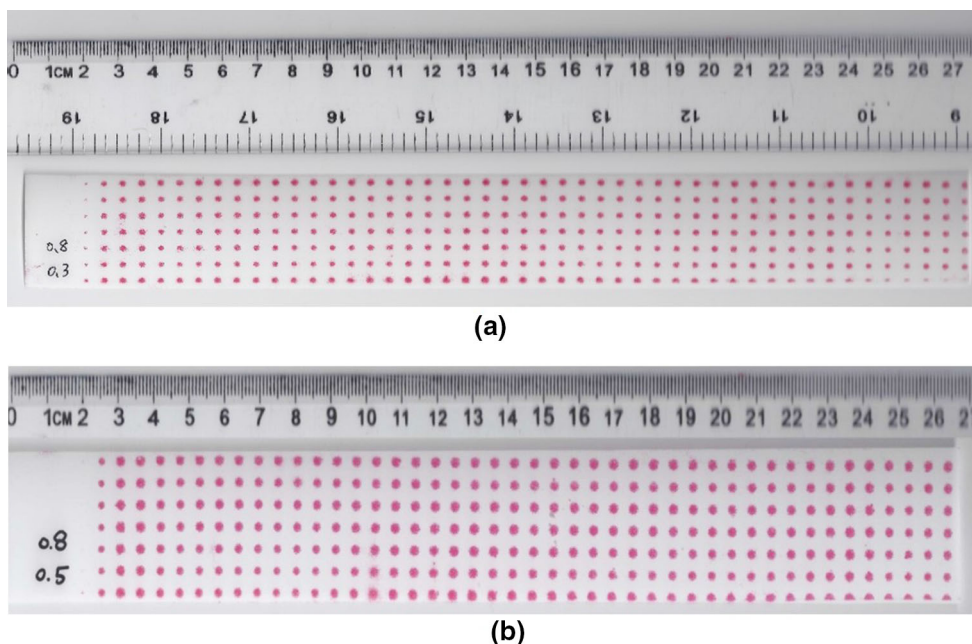


Fig. 8 The measured pressure during rolling imprinting using systems with a gas-bag roller and b rigid roller

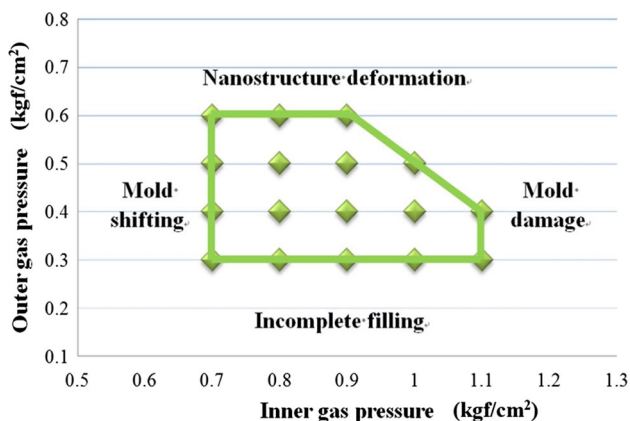


Fig. 9 The operational window of the gas-bag roller-assisted UV-based PDMS roller imprinting for successful fabrication of AAO micro/nano-structures

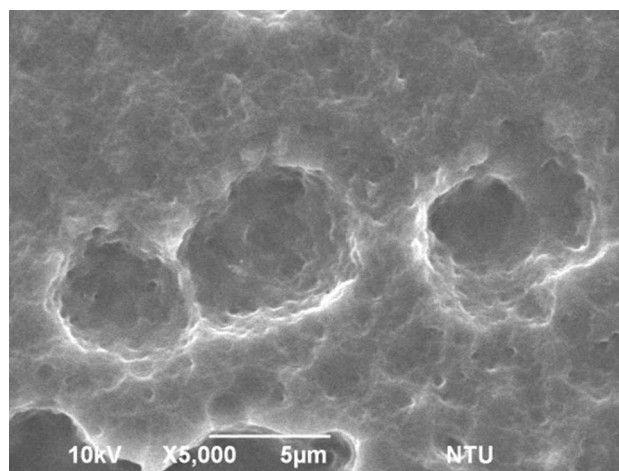


Fig. 10 AAO micro/nano-structures on the fabricated PC film

reflectance of the PC film coated with UV resin is in the range of 6–26%, averaging 17.74%. The average reflectance of the PC film is 2.03% with micro/nano-structures fabricated with an inner gas pressure of 0.8 kgf/cm<sup>2</sup> and outer gas pressure of 0.5 kgf/cm<sup>2</sup>. Figure 12 shows the anti-reflection film under the fluorescent light. Under the same circumstances, the bare PC film has strong reflection. On the contrary, the PC film with an AAO nanostructure is almost free of reflection and is highly transparent.

The hydrophobicity of the PC film with micro/nano-structures is shown in Fig. 13. The contact angle of the bare PC film is 77.5°. With micro/nano-structures, the contact angle increases. The contact angles measured in the PC films with micro/nano-structures are fabricated with the

same inner gas pressure of 0.8 kgf/cm<sup>2</sup>, but with different outer gas pressures. Since the high outer pressure provides high imprinting pressure, which drives the UV resin deeper into the nano pores, the hydrophobicity improves as the outer pressure increases. A contact angle as high as 124.5° is reached.

### 4 Conclusion

In this study, an UV rolling fabrication system of polymeric film with micro/nano-structures using gas-bag-sustained seamless PDMS mold is reported. The seamless PDMS roller mold is cast from the inner wall of an AAO

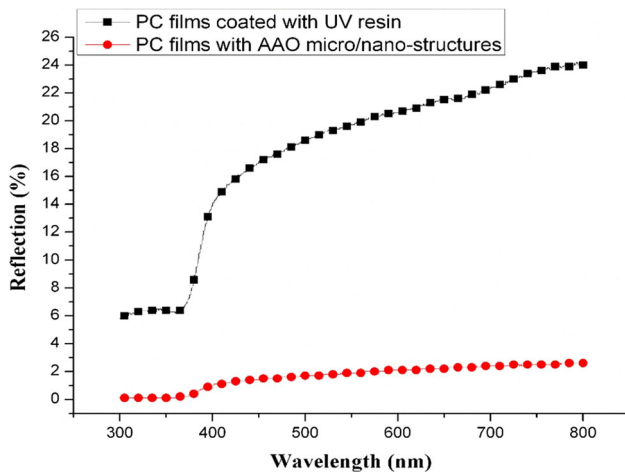


**Fig. 11** The measured reflection of fabricated PC films with AAO micro/nano-structures and of bare PC film in the wavelength of visible light

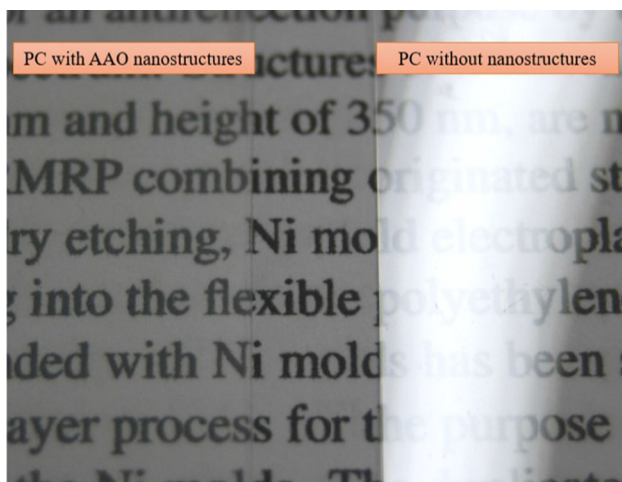


**Fig. 12** Anti-reflection effects as viewed under fluorescent light (left: through a PC film with fabricated AAO micro/nano-structures; right: through a bare PC film)

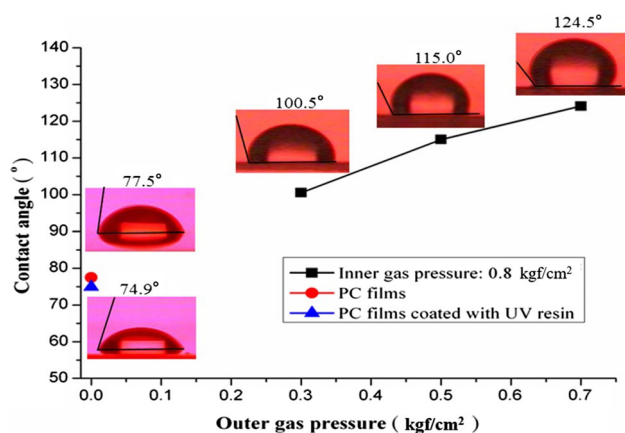


**Fig. 13** The contact angles on PC films with AAO micro/nano-structures fabricated with different outer gas pressures

tube with a two-step anodization process. Further, the PDMS roller mold without seams made the imprinted pattern more successful with no defects on it. The system shows significant improvement in enlarged contact length and uniform pressure between the mold and the substrate, as verified with pressure sensitive film. Successful fabrications of AAO micro/nano-structures on polycarbonate films were achieved. The substantial enhancements in anti-refraction and hydrophobicity in such films have been evaluated. These results show the great potential of the gas-bag roller-sustained seamless PDMS roller mold UV-based rolling imprinting for rapid mass production of micro, nano, and micro/nano-structures.

**References**

Ahn SH, Guo LJ (2009) Large-area roll-to-roll and roll-to-plate nanoimprint lithography: a step toward high-throughput application of continuous nanoimprinting. *ACS Nano* 3:2304–2310. <https://doi.org/10.1021/nn9003633>

Ahn S, Cha J, Myung H, Kim S, Kang S (2006) Continuous ultraviolet roll nanoimprinting process for replicating large-scale nano- and micropatterns. *Appl Phys Lett* 89:213101. <https://doi.org/10.1063/1.2392960>

Ahn SH, Kim J-S, Guo LJ (2007) Bilayer metal wire-grid polarizer fabricated by roll-to-roll nanoimprint lithography on flexible plastic substrate. *J Vac Sci Technol B Microelectron Nanometer Struct Process Meas Phenom* 25:2388–2391. <https://doi.org/10.1116/1.2798747>

Bantz KC, Meyer AF, Wittenberg NJ, Im H, Kurtuluş Ö, Hoon Lee S, Lindquist NC, Oh S-H, Haynes CL (2011) Recent progress in SERS biosensing. *Phys Chem Chem Phys* 13:11551–11567. <https://doi.org/10.1039/C0CP01841D>

Chuang CH, Lee WY, Chuang FF (2013) Fabrication of large area sub-wavelength structure for anti-reflection and self-cleaning optical plate. In: 2013 Symp. Des. Test Integr. Packag. MEMSMOEMS DTIP, pp 1–6

Dumond JJ, Mahabadi KA, Yee YS, Tan C, Fuh JYH, Lee HP, Low HY (2012) High resolution UV roll-to-roll nanoimprinting of resin moulds and subsequent replication via thermal nanoimprint lithography. *Nanotechnology* 23:485310. <https://doi.org/10.1088/0957-4484/23/48/485310>

Fei K, Chiu CP, Hong CW (2008) Molecular dynamics prediction of nanofluidic contact angle offset by an AFM. *Microfluid Nanofluidics* 4:321. <https://doi.org/10.1007/s10404-007-0187-y>

Gale MT (1997) Replication techniques for diffractive optical elements. *Microelectron Eng* 34:321–339. [https://doi.org/10.1016/S0167-9317\(97\)00189-5](https://doi.org/10.1016/S0167-9317(97)00189-5)

Guldin S, Kohn P, Stefik M, Song J, Divitini G, Ecarla F, Ducati C, Wiesner U, Steiner U (2013) Self-cleaning antireflective optical coatings. *Nano Lett* 13:5329–5335. <https://doi.org/10.1021/nl402832u>

Hwang S-K, Jeong S-H, Hwang H-Y, Lee O-J, Lee K-H (2002) Fabrication of highly ordered pore array in anodic aluminum oxide. *Korean J Chem Eng* 19:467–473. <https://doi.org/10.1007/BF02697158>

Lee H, Hong S, Yang K, Choi K (2006) Fabrication of 100 nm metal lines on flexible plastic substrate using ultraviolet curing nanoimprint lithography. *Appl Phys Lett* 88:143112. <https://doi.org/10.1063/1.2193653>

- Mäkelä T (2008) Continuous Double-Sided Roll-to-Roll Imprinting of Polymer Film. *Jpn J Appl Phys* 47:5142. <https://doi.org/10.1143/JJAP.47.5142>
- Marmur A (2008) From hydrophilic to superhydrophobic: theoretical conditions for making high-contact-angle surfaces from low-contact-angle materials. *Langmuir* 24:7573–7579. <https://doi.org/10.1021/la800304r>
- Matschuk M, Larsen NB (2013) Injection molding of high aspect ratio sub-100 nm nanostructures. *J. Micromech Microeng* 23:025003. <https://doi.org/10.1088/0960-1317/23/2/025003>
- Nanayakkara YS, Perera S, Bindiganavale S, Wanigasekara E, Moon H, Armstrong DW (2010) The effect of AC frequency on the electrowetting behavior of ionic liquids. *Anal Chem* 82:3146–3154. <https://doi.org/10.1021/ac9021852>
- Päivänranta B, Baroni P-Y, Scharf T, Nakagawa W, Kuittinen M, Herzig HP (2008) Antireflective nanostructured microlenses. *Microelectron Eng* 85:1089–1091. <https://doi.org/10.1016/j.mee.2008.01.011>
- Park S, Choi K, Kim G, Lee J (2009) Nanoscale patterning with the double-layered soft cylindrical stamps by means of UV-nanoimprint lithography. *Microelectron Eng* 86:604–607. <https://doi.org/10.1016/j.mee.2008.12.074>
- Poinern GEJ, Ali N, Fawcett D (2011) Progress in nano-engineered anodic aluminum oxide membrane development. *Materials* 4:487–526. <https://doi.org/10.3390/ma4030487>
- Tan H, Gilbertson A, Chou SY (1998) Roller nanoimprint lithography. *J Vac Sci Technol B Microelectron Nanometer Struct Process Meas Phenom* 16:3926–3928. <https://doi.org/10.1116/1.590438>
- Thompson GE (1997) Porous anodic alumina: fabrication, characterization and applications. *Thin Solid Films* 297:192–201. [https://doi.org/10.1016/S0040-6090\(96\)09440-0](https://doi.org/10.1016/S0040-6090(96)09440-0)
- Unno N, Taniguchi J (2011) Fabrication of the metal nano pattern on plastic substrate using roll nanoimprint. *Microelectron Eng* 88:2149–2153. <https://doi.org/10.1016/j.mee.2011.02.006>
- Wen J, Shen Z, Qiu Z, Jiang A, Liu R, Chen Y (2011) Fabrication of complex nanostructures of Poly(vinylidene fluoride-trifluoroethylene) by dual step hot-embossing. *J Vac Sci Technol B Nanotechnol Microelectron Mater Process Meas Phenom* 29:06FG08. <https://doi.org/10.1116/1.3662087>
- Wu J-T, Yang S-Y (2010) A gas-bag roller-assisted UV imprinting technique for fabrication of a microlens array on a PMMA substrate. *J Micromech Microeng* 20:085038. <https://doi.org/10.1088/0960-1317/20/8/085038>